Gas-Phase Properties and Reactivity of the Acetate Radical Anion. Determination of the C−H Bond Strengths in Acetic Acid and Acetate Ion

Paul G. Wenthold and Robert R. Squires*

Contribution from The Department of Chemistry, Purdue University, West Lafayette, Indiana 47907

Received July 8, 1994[⊗]

Abstract: The acetate radical anion, $CH_2CO_2^{\bullet -}$, has been generated in the gas phase at room temperature and its thermochemical properties and reactivity have been examined with use of a flowing afterglow−triple quadrupole instrument. This ion is formed in high yield from the reaction between F_2 and the enolate ions of either acetic acid or trimethylsilyl acetate. Collision-induced dissociation (CID) of $CH_2CO_2^{\bullet -}$ occurs by loss of CO_2, forming $CH_2^{\bullet -}$ with a measured threshold energy of 60.9 ± 2.7 kcal/mol. The (oxygen) proton affinity of $CH_2CO_2^{\bullet -}$ (ΔH_{acid}[$^{\bullet}CH_2CO_2$−**H**]) has been determined to be 347.0 ± 1.1 kcal/mol from measurements of the relative yields of the carboxylate ion fragments resulting from CID of proton-bound dimer ions formed by termolecular association of $CH_2CO_2^{\bullet -}$ with carboxylic acids with known gas-phase acidities (i.e., by the Cooks kinetic method). This result indicates that removal of a hydrogen atom from the α-carbon of acetic acid ($\Delta H_{acid}(CH_3CO_2H)$ = 348.6 ± 2.9 kcal/mol) increases the acidity by 1.6 kcal/mol. These data are used to derive the 298 K heat of formation for acetate radical anion, $\Delta H_{f,298}(CH_2CO_2^{\bullet -})$ = −78.2 ± 2.7 kcal/mol, and the C−H bond dissociation energies D_{298}[$^{-}O_2CCH_2$−H] = 93.7 ± 4.0 kcal/mol and D_{298}[HO_2CCH_2−H] = 95.3 ± 2.9 kcal/mol. The acetate radical anion undergoes gas-phase reactions with NO, SO_2, and NO_2 by $CH_2^{\bullet -}$ transfer, forming CH_2NO^-, $CH_2SO_2^{\bullet -}$, and $CH_2NO_2^-$, respectively, and reacts with CH_3SSCH_3 by CH_3S abstraction. Hydrogen atom transfer is shown to occur during the formation of cluster ions of $CH_2CO_2^{\bullet -}$ with certain carboxylic acids.

Introduction

The acetate radical anion, $CH_2CO_2^{\bullet -}$ (**1**), is a prototype cross-conjugated organic radical anion that was first observed by ESR in γ-radiolysis experiments with crystalline glycine more than 30 years ago.[1] Ion **1** has also been produced by radiolysis of

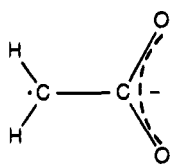

1

aqueous acetate solutions[2] and crystalline acetate salts[3] and by reactions of OH and other free radicals with acetate ion and α-haloacetates.[4] It has also served as a useful paradigm for studies of radical spin polarization (CIDEP),[5] electron−nuclear double resonance (ENDOR),[6] and spin-trapping kinetics.[7] Although the acetate radical anion has been observed as an abundant fragment ion from collision-induced dissociation of aliphatic carboxylate ions[8] and α-substituted acetate ions,[9] its gas-phase chemistry has not been explored.

We recently described a new method for generating biradical negative ions ("distonic" radical anions) in the gas phase from the reaction of molecular fluorine with trimethylsilyl-substituted carbanions.[10] In this paper, we report the generation of acetate radical anion **1** under flowing afterglow conditions from the reaction between F_2 and the enolate ions of acetic acid (eq 1) and trimethylsilyl acetate (eq 2). The gas-phase reactivity of

$$(CH_3)_3Si{-}CH_2CO_2H \xrightarrow{F^-} {}^{-}CH_2CO_2H \xrightarrow{F_2} CH_2CO_2^{\bullet -} \quad (1)$$

$$CH_3CO_2Si(CH_3)_3 \xrightarrow{OH^-} {}^{-}CH_2CO_2Si(CH_3)_3 \xrightarrow{F_2} CH_2CO_2^{\bullet -} \quad (2)$$

$CH_2CO_2^{\bullet -}$ is examined and compared with that of the acetate

[⊗] Abstract published in *Advance ACS Abstracts*, December 1, 1994.

(1) (a) Gordy, W.; Ard, W. B.; Shields, H. *Proc. Natl. Acad. Sci. U.S.A.* **1955**, *41*, 983. (b) Symons, M. C. R. *J. Chem. Soc.* **1959**, 277. (c) Ghosh, D. K.; Whiffen, D. H. *Ibid.* **1960**, 1869. (d) Weiner, R. F.; Koski, W. S. *J. Am. Chem. Soc.* **1963**, *85*, 873. (e) Morton, J. R. *J. Am. Chem. Soc.* **1964**, *86*, 2325.

(2) (a) Neta, P.; Simic, M.; Hayon, E. *J. Phys. Chem.* **1969**, *73*, 4207. (b) Abramovitch, S. D.; Rabani, J. *J. Phys. Chem.* **1976**, *80*, 1562. (c) Sehested, K.; Holcman, J.; Bjergbakke, E.; Hart, E. J. *J. Phys. Chem.* **1987**, *91*, 2359.

(3) Mach, K.; Vacek, K. *Coll. Czech. Chem. Commun.* **1983**, *48*, 203.

(4) (a) Ashworth, B.; Davies, M. J.; Gilbert, B. C.; Norman, R. O. C. *J. Chem. Soc., Perkin Trans. 2* **1983**, 1755. (b) Davies, M. J.; Gilbert, B. C.; Thomas C. B.; Young, J. *J. Chem. Soc., Perkin Trans. 2* **1985**, 1199.

(5) (a) Trifunac, A. D.; Norris, J. R.; Lawler, R. G. *J. Chem. Phys.* **1979**, *71*, 4380. (b) Nuttall, R. H. D.; Trifunac, A. D. *J. Phys. Chem.* **1982**, *86*, 3963. (c) Bartels, D. M.; Lawler, R. G.; Trifunac, A. D. *J. Chem. Phys.* **1985**, *83*, 2686. (d) Syage, J. A. *J. Chem. Phys.* **1987**, *87*, 1033. (e) Bartels, D. M.; Trifunac, A. D.; Lawler, R. G. *Chem. Phys. Lett.* **1988**, *152*, 109.

(6) (a) Brustolon, M.; Maniero, A. L.; Segre, U. *Mol. Phys.* **1988**, *65*, 447. (b) Atherton, N. M.; Oliver, C. E. *J. Chem. Soc., Faraday Trans. 1* **1988**, *84*, 3257.

(7) (a) Madden, K. P.; Taniguchi, H.; Fessenden, R. W. *J. Am. Chem. Soc.* **1988**, *110*, 2753. (b) Meyerstein, D.; Schwarz, H. A. *J. Chem. Soc., Faraday Trans. 1* **1988**, *84*, 2933. (c) Madden, K. P.; Taniguchi, H. *J. Am. Chem. Soc.* **1991**, *113*, 5541.

(8) (a) Jensen, N. J.; Tomer, K. B.; Gross, M. L. *J. Am. Chem. Soc.* **1985**, *107*, 1863. (b) Stringer, M. B.; Bowie, J. H.; Eichinger, C. H.; Currie, G. J. *J. Chem. Soc., Perkin Trans 2* **1987**, 385. (c) Graul, S. T.; Squires, R. R. *J. Am. Chem. Soc.* **1990**, *112*, 2506.

(9) (a) Graul, S. T.; Squires, R. R. *Int. J. Mass Spectrom. Ion Processes* **1990**, *100*, 785. (b) Eichinger, P. C. H.; Bowie, J. H. *Int. J. Mass Spectrom. Ion Processes* **1991**, *110*, 123.

(10) Wenthold, P. G.; Hu, J.; Squires, R. R. *J. Am. Chem. Soc.* **1994**, *116*, 6961.

0002-7863/94/1516-11890$04.50/0

ion. Measurements of the threshold energy for collision-induced dissociation of **1** are described, along with a quantitative determination of its gas-phase proton affinity. These data are used to derive the absolute heat of formation of **1** and the C−H bond dissociation energies in acetic acid and the acetate anion.

Experimental Section

All experiments were carried out with a flowing afterglow−triple quadrupole instrument that has been described in detail previously.[11] Pure helium buffer gas was used in the room-temperature (296 ± 2 K) flow reactor with a total pressure and flow rate of 0.4 Torr and 190 STP cm^3/s, respectively. Fluoride ions and hydroxide ions were generated in the upstream ion source by electron ionization of NF_3 and a N_2O/CH_4 mixture, respectively. The enolate ion of acetic acid was produced by fluoride-induced desilylation of α-trimethylsilylacetic acid (eq 1),[12] while the enolate ion of trimethylsilyl acetate was formed in the flow tube by proton abstraction from the neutral ester, added as the neat vapor through a downstream inlet valve (eq 2). Reaction of either enolate ion with F_2 (5% mixture in helium) yields acetate radical **1**, *m/z* 58, as the major product ion. Several cluster ions are also observed due to HF impurity in the F_2/helium mixture.

Mass analysis and collision-induced dissociation (CID) of ions in the flow tube were carried out with an EXTREL triple quadrupole analyzer located behind a 1 mm sampling orifice in a differentially-pumped chamber. CID of mass-selected ions was performed with argon collision gas in the rf-only, gas-tight central quadrupole (Q2). Target gas pressures corresponding to single-collision conditions (0.04 mTorr) were used for the threshold energy measurements, and somewhat higher pressures (0.10 mTorr) were employed for the cluster ion CID experiments.[11] The reactant ion axial kinetic energy is determined by the Q2 rod-offset voltage, and the energy axis origin and beam energy spread were evaluated by retarding potential analysis, with Q2 serving as the retarding field element. The uncertainty in the beam energy origin is *ca.* 0.1 V. The ion beam energy distributions are approximately Gaussian in shape, with a typical full-width at half-maximum (fwhm) of 0.5−1.5 V.

Threshold energies for CID reactions were determined by the procedures described in several recent publications from this laboratory.[13] For these experiments, the normalized product ion yield or CID cross section is monitored as a function of the axial kinetic energy of the mass-selected reactant ion. Ion appearance curves are constructed by plotting the CID cross section *versus* the collision energy in the center-of-mass frame, $E_{CM} = E_{lab}[m/(m + M)]$, where E_{lab} is the laboratory collision energy and m and M are the masses of the neutral target and reactant ion, respectively. Analysis of the appearance curves is carried out by fitting the experimental data with the assumed model function shown in eq 3, where $\sigma(E)$ is the cross section at energy E, E_T

$$\sigma(E) = \sigma_o \sum [g_i(E + E_i - E_T)^n/E] \qquad (3)$$

is the threshold energy, σ_o is a scaling factor, and n is an adjustable parameter.[13,14] The index i denotes reactant ion vibrational states having energy E_i and population g_i ($\sum g_i = 1$). Absolute cross sections for formation of a single product from CID (σ_p) are calculated using $\sigma_p = I_p/INl$, where I_p and I are the intensities of the product and reactant ions, respectively, N is the number density of the target gas, and l is the effective collision path length (24 ± 4 cm).[11] The model excitation function is convoluted with several distribution functions to account for collision energy broadening in the threshold region. The ion kinetic energy distribution is approximated by a Gaussian distribution with a fwhm of 1.5 eV (lab frame), and the Doppler broadening due to target motion is accounted for by the method of Chantry.[15] The data are fit using an iterative procedure in which E_T, σ_o, and n are varied so to minimize the deviation between the model function and the steeply rising portion of the normalized appearance curve.[16] The region near the reaction onset is not included in the fit due to tailing in the data that is caused by the ill-defined effects of collisional activation outside of the collision cell. Analysis of the data for the present systems was also carried out with a modified form of the model function which explicitly accounts for kinetic shifts in the dissociation onsets.[13] However, these effects were found to be negligibly small ($\Delta E_T < 0.02$ eV). Because of the explicit inclusion of the reactant ion thermal energy content in the fitting procedure, the CID threshold energy obtained with use of eq 3 corresponds to the 0 K dissociation energy, i.e. D_0. The corresponding D_{298} values are obtained by adding the difference in integrated heat capacities for the products and reactants (obtained from semiempirical MO calculations[17]). For deriving 298 K heats of formation, an additional factor of RT (0.59 kcal/mol), corresponding to the PV work term for dissociation, is also added to convert D_{298} to an enthalpy change, DH_{298}.

Gas purities were as follows: helium (99.995%), argon (99.998%), nitrogen dioxide (99.5%), nitric oxide (99%), and sulfur dioxide (99.98%). Acetic acid-d_3 was prepared by H/D exchange of CD_3CO_2D (Aldrich, 99.5% d_4) in dilute NaOH solution. All other reagents were obtained from commercial sources and used as supplied other than degassing just prior to use.

Scheme 1

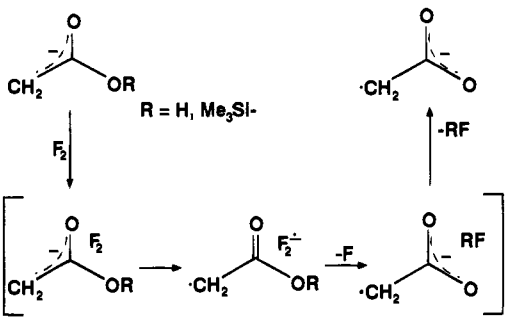

Results and Discussion

The acetate radical anion **1** is observed as an intense signal at *m/z* 58 in the mass spectrum that results from reaction of F_2 with the enolate ion of either acetic acid (eq 1) or its trimethylsilyl ester (eq 2). These reactions are believed to occur by dissociative electron transfer from the organic ion to F_2 to form F^- in the initial enolate/F_2 collision complex, followed by either F^--induced desilylation of the ester moiety or proton transfer to F^- from the carboxylic acid group (Scheme 1).[10] Acetate ion, $CH_3CO_2^-$, *m/z* 59, is formed as an abundant side product in both reaction sequences, and fluoroacetate ion, $FCH_2CO_2^-$, *m/z* 77, is also formed as a secondary reaction product. For chemical studies and CID threshold analysis, reaction 1 provides the most efficient synthesis of **1**.

The reactions of **1** with several small molecules were examined in the helium flow reactor. Transfer of $CH_2^{\bullet-}$ was observed to occur with NO, NO_2, and SO_2 (eqs 4−6). Transfer

$$1 + NO \rightarrow CH_2NO^- + CO_2 \qquad (4)$$

(11) (a) Marinelli, P. J.; Paulino, J. A.; Sunderlin, L. S.; Wenthold, P. G.; Poutsma, J. C.; Squires, R. R. *Int. J. Mass. Spectrom. Ion Processes* **1994**, *130*, 89. (b) Graul, S. T.; Squires, R. R. *Mass Spectrom. Rev.* **1988**, *7*, 263.

(12) (a) O'Hair, R. A. J.; Gronert, S.; DePuy, C. H.; Bowie, J. H. *J. Am. Chem. Soc.* **1989**, *111*, 3105. (b) Grabowski, J. J.; Cheng, X. *J. Am. Chem. Soc.* **1989**, *111*, 3106.

(13) (a) Sunderlin, L. S.; Wang, D.; Squires, R. R. *J. Am. Chem. Soc.* **1992**, *114*, 2788. *Ibid.* **1993**, *115*, 12060. (b) Wenthold, P. G.; Squires, R. R. *J. Am. Chem. Soc.* **1994**, *116*, 6401. (c) Wenthold, P. G.; Wierschke, S. G.; Nash, J. J.; Squires, J. J. *J. Am. Chem. Soc.* **1994**, *116*, 7378.

(14) (a) Chesnavich, W. J.; Bowers, M. T. *J. Phys. Chem.* **1979**, *83*, 900. (b) Rebick, C.; Levine, R. D. *J. Chem. Phys.* **1973**, *58*, 3942. (c) Sunderlin, L. S.; Armentrout, P. B. *Int. J. Mass Spectrom. Ion Processes* **1989**, *94*, 149 and references therein.

(15) Chantry, P. J. *J. Chem. Phys.* **1971**, *55*, 2746.

(16) Data analysis carried out using the CRUNCH program developed by P. B. Armentrout and co-workers.

(17) AM1: Dewar, M. J. S.; Zoebisch, E. G.; Healy, E. F.; Stewart, J. J. P. *J. Am. Chem. Soc.* **1985**, *107*, 3902. MOPAC: Stewart, J. J. P. QCPE No. 455.

$$1 + NO_2 \rightarrow CH_2NO_2^- + CO_2 \quad (5)$$

$$1 + SO_2 \rightarrow CH_2SO_2^{\bullet -} + CO_2 \quad (6)$$

of $CH_2^{\bullet -}$ to NO is also observed with the related cross-conjugated radical anions $C(CH_2)_3^{\bullet -}$ [10] and $CH_2C(O)CH_2^{\bullet -}$.[18] Its occurrence with both open-shell molecules such as NO and NO_2 and closed-shell molecules such as SO_2 indicates that it is not necessarily a radical-mediated process, since all three neutral reactants can behave as Lewis acids. Although the simple adducts of **1** with SO_2 and NO are not observed, even at pressures in the flow reactor up to 0.45 Torr, the reaction of **1** with NO_2 proceeds by termolecular addition as well as $CH_2^{\bullet -}$ transfer. This provides evidence that adducts are short-lived intermediates in the transfer reactions. Products arising from $O^{\bullet -}$ transfer are not observed in these reactions, although their formation is predicted to be exothermic by *ca.* 15 kcal/mol for the reaction with NO_2 (eq 5) and near thermoneutral for the reactions with NO and SO_2 (eqs 4 and 6, respectively).[19] An ion that is isoelectronic with **1**, $CO_3^{\bullet -}$, is known to react with to NO,[20] NO_2,[21] and SO_2[20] by $O^{\bullet -}$ transfer to form NO_2^-, NO_3^-, and $SO_3^{\bullet -}$, respectively.

Kenttämaa and co-workers have developed a variety of chemical methods based on radical-type reactions for use in detecting the presence of distonic radical *cation* structures in the gas phase,[22] such as methylthio (CH_3S) group abstraction from CH_3SSCH_3[23] and iodine atom transfer from alkyl iodides.[24] We have examined the behavior of **1** toward some of these reagents. Acetate radical anion reacts slowly with CH_3S-SCH_3 to form the CH_3S abstraction product and CH_3S^- (eq 7).

$$1 + CH_3SSCH_3 \rightarrow CH_3SCH_2CO_2^- + CH_3S$$
$$\rightarrow CH_3S^- + [3C, 5H, 2O, S] \quad (7)$$

Acetate ion is completely unreactive toward CH_3SSCH_3, suggesting that methylthio group abstraction by **1** involves a radical mechanism. Although CH_3S^- has been observed as a product from gas-phase reactions between CH_3SSCH_3 and relatively strong-base, even-electron negative ions,[25] it is not expected to form with the weakly basic ion **1** (*vide infra*). The structure of the neutral product(s) that accompany CH_3S^- are unknown. No ionic products attributable to iodine atom transfer are observed from reaction of **1** with either CH_3I or $(CH_3)_2CHI$. However, I^- is formed as an abundant product, presumably by means of a nucleophilic displacement reaction. Hydrogen atom transfer to **1** is also conspicuously absent, even in cases where it should be thermodynamically favorable (*vide infra*), such as with dimethyl ether ($D[CH_3OCH_2-H]$ = 93 kcal/mol[26]), toluene

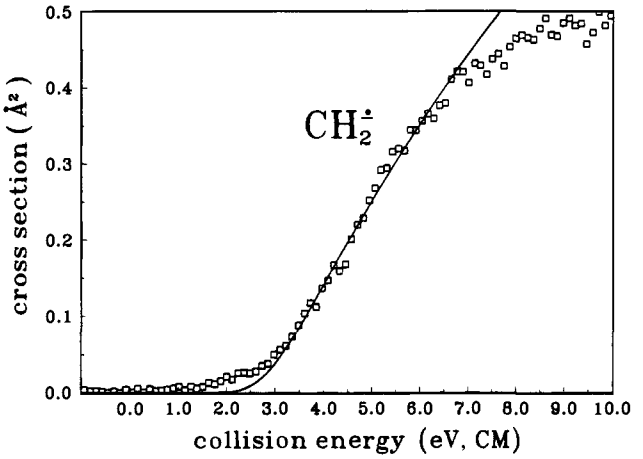

Figure 1. Cross sections for collision-induced decarboxylation of $CH_2CO_2^{\bullet -}$ as a function of translational energy in the center-of-mass frame. The solid line is the model appearance curve calculated using eq 3 as discussed in the text.

($D[PhCH_2-H]$ = 88.5 kcal/mol[27]), and 1,3-cyclohexadiene ($D[C_6H_7-H]$ = 73 kcal/mol[19]). These results suggest that barriers exist for atom and group transfers to the radical site in **1**; such a proposal has been made previously to explain the low radical reactivity exhibited by certain distonic radical cations.[24a]

Collisional activation of **1** in the triple quadrupole with argon target in the 1−20 eV (lab) collision energy range results in dissociation by loss of CO_2, forming $CH_2^{\bullet -}$ (eq 8). The reaction

$$CH_2CO_2^{\bullet -} \xrightarrow{CID} CH_2^{\bullet -} + CO_2 \quad (8)$$

is relatively inefficient, with a maximum total cross section of 0.5 Å^2 at 10 eV (CM). The measured appearance curve for $CH_2^{\bullet -}$ is shown in Figure 1, along with the convoluted fit of the data with the model function given by eq 3. The derived threshold energy for CID, E_T, obtained from replicate measurements is 2.64 ± 0.12 eV (60.9 ± 2.7 kcal/mol), where the indicated uncertainty includes the precision of the data (0.10 eV), the uncertainty in the energy scale (0.06 eV), and a 0.02 eV uncertainty to allow for the possibility of a kinetic shift. The measured threshold energy for this dissociation formally represents an upper limit to the actual bond dissociation energy, $D_0[CH_2^{\bullet -}-CO_2]$. However, previous studies of the decarboxylation reactions of a wide variety of carboxylate ions[28] have shown a good correspondence between the measured CID thresholds and the reaction endothermicities. Moreover, there is no reason to expect that the reverse of reaction 8, nucleophilic addition of $CH_2^{\bullet -}$ to CO_2, would have an energy barrier since theoretical[29] and experimental[30] studies of the reactions of CO_2 with anions having basicities similar to that of $CH_2^{\bullet -}$ ($\Delta H_{acid}(CH_3)$ = 409.1 ± 0.5 kcal/mol[19]) indicate that such barriers are absent. Therefore, the measured threshold for CID of **1**, E_T, is taken to be a good estimate for D_0. The corresponding enthalpy change, $DH_{298}[CH_2^{\bullet -}-CO_2]$ is determined from the measured threshold energy to be 62.3 ± 2.7 kcal/mol.

For comparison, the measured cross sections for CID of acetate ion (eq 9) are presented in Figure 2. Analysis of the

(18) Wenthold, P. G.; Squires, R. R. Unpublished results.
(19) Lias, S. G.; Bartmess, J. E.; Liebman, J. F.; Holmes, J. L.; Levin, R. D.; Mallard, W. D. *J. Phys. Chem. Ref. Data* **1988**, *17*, Suppl. 1. All data taken from the NIST Negative Ion Energetics Database, Version 3.00, NIST Standard Reference Database 19B, October 1993.
(20) Albritton, D. L.; Dotan, I.; Streit, G. E.; Fahey, D. W; Fehsenfeld, F. C.; Ferguson, E. E. *J. Chem. Phys.* **1983**, *78*, 6614.
(21) Sieck, L. W.; Swarles, S. K. *J. Am. Chem. Soc.* **1970**, *92*, 2937.
(22) Stirk, K. M.; Kiminkinen, L. K. M.; Kenttämaa, H. I. *Chem. Rev.* **1992**, *92*, 1649.
(23) Stirk, K. M.; Orlowski, J. C.; Leeck, D. T.; Kenttämaa, H. I. *J. Am. Chem. Soc.* **1992**, *114*, 8604.
(24) (a) Smith, R. L.; Chyall, L. J.; Stirk, K. M.; Kenttämaa, H. I. *Org. Mass Spectrom.* **1993**, *28*, 1623. (b) Kenttämaa, H. I. *Org. Mass Spectrom.* **1994**, *29*, 1. (c) Stirk, K. M.; Smith, R. L.; Orlowski, J. C.; Kenttämaa, H. I. *Rapid Commun. Mass Spectrom.* **1993**, *7*, 392. (d) Chyall, L. J.; Kenttämaa, H. I. *J. Am. Chem. Soc.* **1994**, *116*, 3135.
(25) Grabowski, J. J.; Zhang, L. *J. Am. Chem. Soc.* **1989**, *111*, 1193.
(26) McMillen, D. F.; Golden, D. M. *Annu. Rev. Phys. Chem.* **1982**, *33*, 493.
(27) Berkowitz, J.; Ellison, G. B.; Gutman, D. *J. Phys. Chem.* **1994**, *98*, 2744.
(28) Graul, S. T.; Squires, R. R. *J. Am. Chem. Soc.* **1992**, *114*, 2517.
(29) Liang, J.; Lipscomb, W. N. *J. Am. Chem. Soc.* **1986**, *108*, 5051 and references therein.
(30) (a) Bierbaum, V. M.; DePuy, C. H.; Shapiro, R. H. *J. Am. Chem. Soc.* **1977**, *99*, 5800. (b) Bierbaum, V. M.; Grabowski, J. J.; DePuy, C. H. *J. Phys. Chem.* **1984**, *88*, 1389. (c) DePuy, C. H. *Org. Mass Spectrom.* **1985**, *20*, 556. (d) Squires, R. R. *Int. J. Mass Spectrom. Ion Processes* **1992**, *117*, 565.

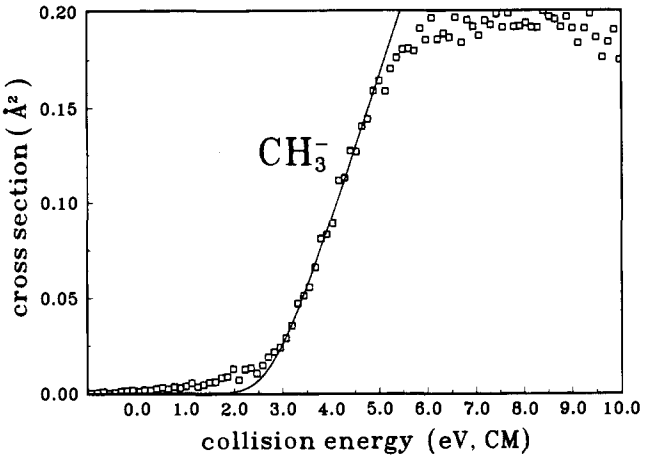

Figure 2. Cross sections for collision-induced decarboxylation of $CH_3CO_2^-$ as a function of translational energy in the center-of-mass frame. The solid line is the model appearance curve calculated using eq 3 as discussed in the text.

Table 1. Supplemental and Derived Thermochemical Data[a]

	heat of formation		
	0 K	298 K	ref
CH_3CO_2H	-99.9 ± 0.1	-103.3 ± 0.1	*b*
$^{\bullet}CH_2CO_2H$	-58.2 ± 2.9	-59.5 ± 2.9	this work
		-61.6 ± 3.0	*c*
		-58.1	*d*
$CH_3CO_2^-$	-117.1 ± 2.9	-120.4 ± 2.9	*e*
$CH_2CO_2^{\bullet-}$	-76.8 ± 2.7	-78.2 ± 2.7	this work
CH_3^-	33.9 ± 0.9	33.1 ± 0.9	*e*
$CH_2^{\bullet-}$	78.1 ± 0.2	78.2 ± 0.2	*e*
CO_2	-94.0 ± 0.1	-94.1 ± 0.1	*f*
H	51.6	52.1	*f*
H^+	365.2	365.7	*e*

	bond dissociation energy		
	0 K	298 K	ref
$D[CH_2^{\bullet-}-CO_2]$	60.9 ± 2.7	61.7 ± 2.7	this work
$D[CH_3^--CO_2]$	57.5 ± 2.5	59.1 ± 2.5	this work
	56.4 ± 3.0	58.8 ± 3.0	*e*
$D[-O_2CCH_2-H]$	91.9 ± 4.0	93.7 ± 4.0	this work
		91.9 ± 1.7	*g*
$D[HO_2CCH_2-H]$	93.3 ± 2.9	95.3 ± 2.9	this work
		93.9 ± 3.0	*c*
		97.3	*d*

	gas-phase acidity (ΔH_{acid})		
	0 K	298 K	ref
$CH_3CO_2-\mathbf{H}$	348.0 ± 2.9	348.6 ± 2.9	*e*
$^{\bullet}CH_2CO_2-\mathbf{H}$	346.6 ± 1.1	347.0 ± 1.1	this work

[a] All data in kcal/mol. [b] Chao, J.; Zwolinski, B. J. *J. Phys. Chem. Ref. Data* **1978**, *7*, 363. [c] Reference 35. [d] Reference 34. [e] Reference 19. [f] Chase, M. W.; Davies, C. A.; Downey, J. R.; Frurip, D. J.; McDonald, R. A.; Syverud, A. N. *J. Phys. CHem. Ref. Data* **1985**, *14*, Suppl. 1 (JANAF Tables). [g] Reference 31.

$$CH_3CO_2^- \xrightarrow{CID} CH_3^- + CO_2 \quad (9)$$

CH_3^- appearance curve with the same method used for **1** gives an average value for the 0 K threshold energy, $D_0[CH_3^--CO_2]$, of 2.50 ± 0.11 eV and a 298 K dissociation enthalpy, $DH_{298}[CH_3^--CO_2]$, of 59.7 ± 2.5 kcal/mol. This latter value is in good agreement with the previously reported value derived from a different analytical procedure (61.6 ± 3.5 kcal/mol[28]) and with the value 59.4 ± 3.0 kcal/mol calculated from the standard 298 K heats of formation of CH_3^-, $CH_3CO_2^-$, and CO_2 listed in Table 1.[19]

The absolute heat of formation for $CH_2CO_2^{\bullet-}$ and the C−H bond dissociation energy in $CH_3CO_2^-$ can be calculated from the CID results and the auxiliary data listed in Table 1 according to eqs 10 and 11. The derived values are $\Delta H^\circ_{f,o}[CH_2CO_2^{\bullet-}]$

$$\Delta H_{f,o}[CH_2CO_2^{\bullet-}] = \Delta H_{f,o}[CH_2^{\bullet-}] + \Delta H_{f,o}[CO_2] - D_0[CH_2^{\bullet-}-CO_2] \quad (10)$$

$$D_0[^-O_2CCH_2-H] = \Delta H_{f,o}[CH_2CO_2^{\bullet-}] + \Delta H_{f,o}[H] - \Delta H_{f,o}[CH_3CO_2^-] \quad (11)$$

$= -76.8 \pm 2.7$ kcal/mol and $D_0[^-O_2CCH_2-H] = 91.9 \pm 4.0$ kcal/mol, where the assigned uncertainties are the square root of the sum of squares of the component uncertainties (Table 1). The corresponding 298 K values are also given in Table 1. The 298 K bond energy derived from this study, 93.7 ± 4.0 kcal/mol, is slightly higher than that obtained from photoacoustic calorimetry (PAC),[31] 91.9 ± 1.7 kcal/mol. Although there is considerable overlap in the uncertainties, the discrepancy is probably real since the α-CH bond energies determined for alcohols in the PAC study are typically 1−2 kcal/mol lower than reported gas-phase values.[31]

The (oxygen) proton affinity of **1**, which is equivalent to $\Delta H_{acid}(^{\bullet}CH_2CO_2-\mathbf{H})$,was determined by the Cooks kinetic method.[32] This tandem mass spectrometric procedure has been shown to provide accurate values for gas-phase acidities of carboxylic acids[32,33] and related species, and it is well-suited for the present system since the $^{\bullet}CH_2CO_2H$ radical is too reactive for conventional gas-phase equilibrium acidity measurements. For these experiments, cluster ions ("proton-bound dimers") of the general constitution $[^{\bullet}CH_2CO_2^-\cdots H^+\cdots{}^-O_2CR']$ were formed in the flow tube by allowing **1** to undergo termolecular association reactions with different aliphatic carboxylic acids. The relative yield of the two carboxylates produced by collision-induced dissociation of these cluster ions is a sensitive function of the relative basicities of the fragments and is amenable to calibration using carboxylic acids with known gas-phase acidities. In principle, several different calibration protocols may be employed. A standard curve can be constructed by plotting the logarithm of the measured CID yield ratios for a series of dimer ions comprised of a "fixed reference" acid and several different reference carboxylates (ordinate) *versus* their known gas-phase acidities, $\Delta G_{acid}(RCO_2H)$ (abscissa). The unknown acidity for $^{\bullet}CH_2CO_2H$ is then determined from the calibration plot and the measured CID yield ratio obtained for the proton-bound dimer of $CH_2CO_2^{\bullet-}$ with the reference carboxylic acid. Alternatively, the standard curve can be constructed using the CID yield ratios and the *differences* in the gas-phase acidities of the two reference acids, $\delta\Delta G_{acid}$. A "global" calibration approach can be used in which various combinations of reference acids are employed, such that up to $N!/2$ data points may be determined for N different references. The desired acidity for $^{\bullet}CH_2CO_2H$ is then obtained from the measured CID yield ratios for proton-bound dimers of $CH_2CO_2^{\bullet-}$ with one or more of the reference acids used for the calibration plot. A third possibility is a "multireference approach" wherein $CH_2CO_2^{\bullet-}$ is allowed to form proton-bound dimer ions with a series of carboxylic acids, RCO_2H, having known gas-phase acidities,

(31) Kanabus-Kaminska, J. M.; Gilbert, B. C.; Griller, D. *J. Am. Chem. Soc.* **1989**, *111*, 3311.

(32) (a) Wright, L. G.; McLuckey, S. A.; Cooks, R. G. *Int. J. Mass. Spectrom. Ion Phys.* **1982**, *42*, 115. (b) Hoke, S. H., II; Yang, S. S.; Cooks, R. G.; Hrovat, D. A.; Borden, W. T. *J. Am. Chem. Soc.* **1994**, *116*, 4888. (c) Patrick, J. S.; Kotiaho, T.; McLuckey, S. A.; Cooks, R. G. *Mass Spectrom. Rev.*, submitted for publication.

(33) Graul, S. T.; Schnute, M. E.; Squires, R. R. *Int. J. Mass Spectrom. Ion Processes* **1990**, *96*, 181.

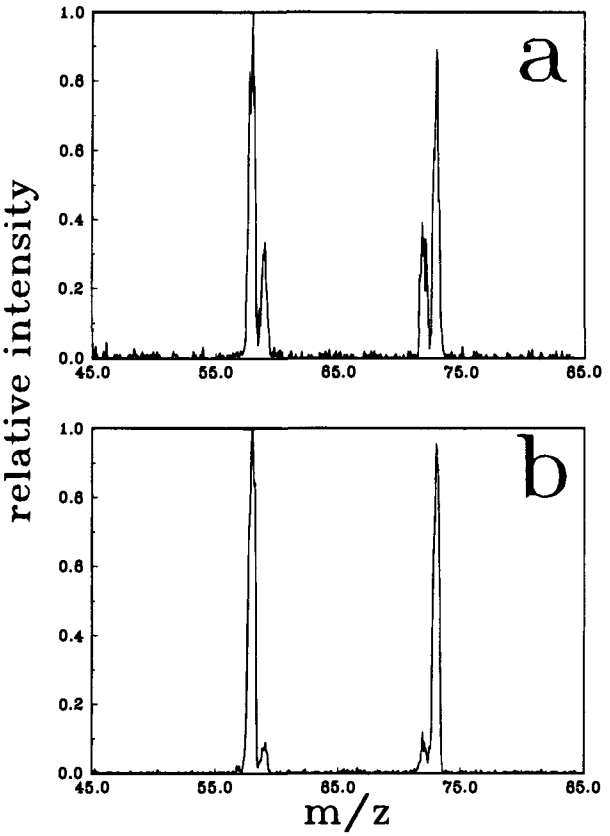

Figure 3. Collision-induced dissociation spectrum (20 eV, lab) for (a) $[CH_2CO_2^{\bullet-}\cdots H^+\cdots {}^-O_2CCH_2CH_3]$ formed by direct association and (b) $[CH_2CO_2^{\bullet-}\cdots H^+\cdots {}^-O_2CCH_2CH_3]$ formed by a "switching" reaction with $[CH_2CO_2^{\bullet-}\cdots CH_3CN]$.

and the CID yield ratios ($R = I(RCO_2^-)/I(CH_2CO_2^{\bullet-})$ are determined for each. The acidity of $^{\bullet}CH_2CO_2H$ is then given by the x-intercept of a plot of ln R (ordinate) *vs* $\Delta G_{acid}(RCO_2H)$ (abscissa).

In the course of applying the above procedures, we found that several of the proton-bound dimer ions formed from **1** produce CID product ions that are derived from an apparent hydrogen atom transfer between the two carboxylate ions. For example, the cluster ion formed from $CH_2CO_2^{\bullet-}$ and propionic acid, $C_2H_5CO_2H$, undergoes CID (Figure 3a) to yield the four product ions shown below (eq 12). The fragment ions with *m/z*

$$\begin{aligned} CH_2CO_2^{\bullet-} + C_2H_5CO_2H &\rightarrow \underset{m/z\ 132}{[C_5H_8O_4]^{\bullet-}} \\ &\xrightarrow{CID} \underset{m/z\ 58}{CH_2CO_2^{\bullet-}} + C_2H_5CO_2H \\ &\rightarrow \underset{m/z\ 59}{CH_3CO_2^-} + {}^{\bullet}C_2H_4CO_2H \\ &\rightarrow CH_3CO_2H + \underset{m/z\ 72}{C_2H_4CO_2^{\bullet-}} \\ &\rightarrow {}^{\bullet}CH_2CO_2H + \underset{m/z\ 73}{C_2H_5CO_2^-} \end{aligned} \quad (12)$$

59 and *m/z* 72 indicate that a hydrogen atom has transferred to $CH_2CO_2^{\bullet-}$ at some point during the formation, lifetime, or decomposition of the cluster ion. The most likely source of the hydrogen atom is the α-carbon in $CH_3CH_2CO_2H$, since the OH bond energy (106 ± 2 kcal/mol)[19] and β-CH bond energy (*ca.* 100 kcal/mol) are considerably larger than the α-CH bond

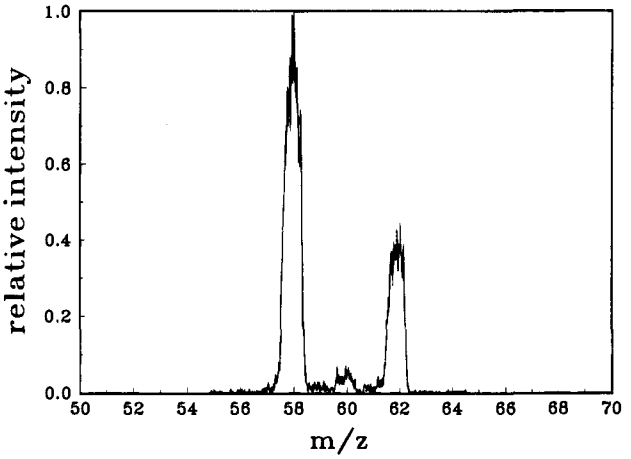

Figure 4. Collision-induced dissociation spectrum (20 eV, lab) for $[CH_2CO_2^{\bullet-}\cdots H^+\cdots {}^-O_2CCD_3]$ formed by direct association.

energy (*ca.* 92 kcal/mol). Indirect support for this comes from the fact that hydrogen atom transfer products are absent from the CID spectra obtained with clusters of **1** with carboxylic acids that do not have α-hydrogens, such as $(CH_3)_3CCO_2H$, or in which the α-CH bond energy is exceptionally high, such as in cyclopropanecarboxylic acid (c-$C_3H_5CO_2H$, $D \approx 98$ kcal/mol).

The H atom transfer from $CH_3CH_2CO_2H$ to **1** occurs either when the cluster first forms, during the lifetime of the cluster prior to CID, or when it decomposes upon collisional activation. One way to distinguish among these possibilities is to form the $CH_3CH_2CO_2H/CH_2CO_2^{\bullet-}$ cluster ion by a "switching" reaction, such that it has an energy below the H atom transfer barrier. This can suppress the reaction during initial cluster formation. An analogous procedure was used recently to demonstrate the occurrence of thermoneutral hydride transfer during the initial formation (but not CID) of $ClCH_2ClCH_3^+$ from $ClCH_2^+ + ClCH_3$.[11a] For the present system, the switching reaction was carried out by first allowing **1** to react with acetonitrile (CH_3CN) in the upstream region of the flow tube, followed by adding $CH_3CH_2CO_2H$ further downstream to effect the displacement of the CH_3CN molecule (eq 13). The cluster ion formed in

$$CH_2CO_2^{\bullet-} \xrightarrow{CH_3CN} [CH_2CO_2^{\bullet-}\cdots CH_3CN] \xrightarrow{CH_3CH_2CO_2H} [CH_2CO_2^{\bullet-}\cdots H^+\cdots {}^-O_2CCH_2CH_3] \quad (13)$$

this way undergoes CID to yield only a small amount of the ions with *m/z* 59 and *m/z* 72, as shown in Figure 3b. This result indicates that most of the hydrogen atom transfer between **1** and $C_2H_5CO_2H$ shown in eq 12 occurs during the initial *formation* of the proton-bound dimer.[11a] The minor yield of fragment ions with *m/z* 59 and 72 appearing in the spectrum shown in Figure 3b is most likely due to reaction between $C_2H_5CO_2H$ and the small amount of unclustered $CH_2CO_2^{\bullet-}$ that remains in the flow reactor even with the highest attainable flows of CH_3CN (*ca.* 0.25 STP cm^3/s).

The CID behavior of the cluster ion produced by reaction between $CH_2CO_2^{\bullet-}$ and CD_3CO_2H provides additional insight into the H atom transfer reaction. The mass spectrum obtained from CID of this cluster ion with argon target under single-collision conditions is shown in Figure 4. The major products are $CH_2CO_2^{\bullet-}$ (*m/z* 58) and $CD_3CO_2^-$ (*m/z* 62), with relative intensities that are consistent with the differing basicities of these two ions (*vide infra*). In addition, a small amount of product with *m/z* 60 is formed, which corresponds to the deuterium atom transfer products, $DCH_2CO_2^-$ and $CD_2CO_2^{\bullet-}$. The appearance of only traces of fragment ions at *m/z* 59 and 61 indicates that multiple H/D exchanges are insignificant.

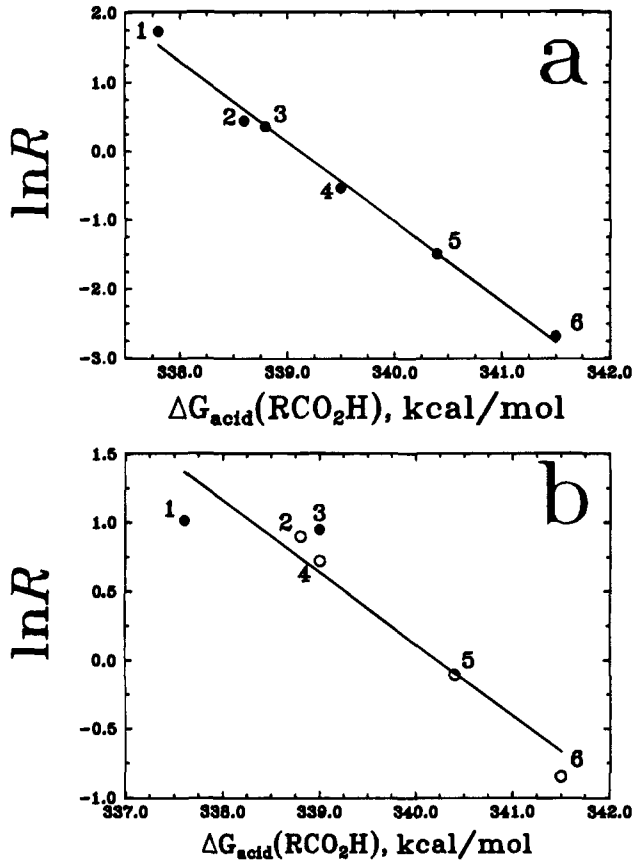

Figure 5. Calibration plots for acidity determination by the kinetic method using (a) a single-reference approach, where $R = I(RCO_2^-)/I(c\text{-}C_3H_5CO_2^-)$ and RCO_2^- refers to (1) $(CH_3)_3CCH_2CO_2^-$, (2) $c\text{-}C_5H_9CO_2^-$, (3) $c\text{-}C_4H_7CO_2^-$, (4) $1\text{-}C_3H_7CO_2^-$, (5) $C_2H_5CO_2^-$, and 6) $CH_3CO_2^-$, and (b) a multiple reference approach, where $R = I(RCO_2^-)/I(CH_2CO_2^{\bullet-})$ and RCO_2^- refers to (1) $(CH_3)_3CCO_2^-$, (2) $c\text{-}C_4H_7CO_2^-$, (3) $c\text{-}C_3H_5CO_2^-$, (4) $2\text{-}C_3H_7CO_2^-$, (5) $C_2H_5CO_2^-$, and (6) $CH_3CO_2^-$. The open circles indicate proton-bound dimers that also yield CID products derived from hydrogen atom transfer.

For the kinetic method experiments involving the single-reference calibration procedure, cyclopropanecarboxylic acid ($c\text{-}C_3H_5CO_2H$) was chosen as the reference acid in order to avoid potentially deleterious effects on the quantitative CID measurements from hydrogen atom transfer. Figure 5a shows a semilog plot of the measured CID yield ratios, $R = I(RCO_2^-)/I(c\text{-}C_3H_5CO_2^-)$, obtained from proton-bound dimer ions formed from $c\text{-}C_3H_5CO_2^-$ and six different aliphatic carboxylic acids *versus* the corresponding ΔG_{acid} values. A linear least-squares analysis of the data gives the relation $\Delta G_{acid} = (339.1 \pm 0.9) - (0.85 \pm 0.58)$ ln R kcal/mol ($r^2 = 0.99$), where the assigned uncertainties are calculated as described in the Appendix. The corresponding effective temperature[32] is 429 ± 290 K. The measured yield ratio obtained from CID of $[CH_2CO_2^{\bullet-}\cdots H^+\cdots {}^-O_2CC_3H_5]$ is 0.388 ± 0.095. Combining this in the regression equation gives a value for $\Delta G_{acid}(^{\bullet}CH_2CO_2H)$ of 339.9 ± 1.0 kcal/mol.

For the multireference calibration experiments, the CID yield ratios, $R = I(RCO_2^-)/I(CH_2CO_2^{\bullet-})$, were determined for six different proton-bound dimer ions of the form $[CH_2CO_2^{\bullet-}\cdots H^+\cdots {}^-O_2CR]$. A plot of ln R *vs* $\Delta G_{acid}(RCO_2H)$ is shown in Figure 5b. Hydrogen atom transfer products are observed in the CID spectra with most of the reference carboxylic acids; these are denoted by open circles in Figure 5b. Regression analysis of these data gives the relation $\Delta G_{acid} = (340.1 \pm 1.0) - (1.72 \pm 1.20)$ ln R kcal/mol ($r^2 = 0.90$) and an effective temperature[32] of 866 ± 604 K. Thus, $\Delta G_{acid}(^{\bullet}CH_2CO_2H)$ is determined by this approach to be 340.1 ± 1.0 kcal/mol. The good linearity of the plot in Figure 5b and the excellent agreement between the acidities determined with the two different procedures indicates that the occurrence of hydrogen atom transfer is not interfering with the normal competitive cleavage of the proton-bound dimers. The average value of $\Delta G_{acid}(^{\bullet}CH_2CO_2H)$ from the two measurements is 340.0 ± 0.7 kcal/mol. A complete description of the procedures used to assign uncertainties to the derived acidities is given in the Appendix.

The corresponding value of $\Delta H_{acid}(^{\bullet}CH_2CO_2H)$ is given by $\Delta G_{acid} + T\Delta S_{acid}$. The entropy of acid dissociation, ΔS_{acid}, is taken to be the same as that assigned to acetic acid, 23.5 ± 3.0 eu,[19] giving a final value for $\Delta H_{acid}(CH_2CO_2H)$ of 347.0 ± 1.1 kcal/mol at 298 K. Thus, removal of a hydrogen atom from the α-carbon in acetic acid ($\Delta H_{acid}(^{\bullet}CH_3CO_2H) = 348.6 \pm 2.9$ kcal/mol)[19] leads to a 1.6 kcal/mol increase in gas-phase acidity (about 1.2 pK_a units at room temperature). This is probably a result of the better π-accepting ability of a $^{\bullet}CH_2$ group compared to a CH_3 group, which leads to greater charge delocalization in $CH_2CO_2^{\bullet-}$ compared to $CH_3CO_2^-$.

The 298 K heat of formation and proton affinity of **1** can be used to derive values for the absolute heat of formation of $^{\bullet}CH_2CO_2H$ and the C−H bond energy in CH_3CO_2H at 298 K according to eqs 14 and 15. Using the measured quantities from

$$\Delta H_{f,298}[^{\bullet}CH_2CO_2H] = \Delta H_{f,298}[CH_2CO_2^{\bullet-}] + \Delta H_{f,298}[H^+] - \Delta H_{acid}[^{\bullet}CH_2CO_2H] \quad (14)$$

$$D_{298}[HO_2CCH_2{-}H] = \Delta H_{f,298}[^{\bullet}CH_2CO_2H] + \Delta H_{f,298}[H] - \Delta H_{f,298}[CH_3CO_2H] - RT \quad (15)$$

this study and the auxiliary thermochemical data listed in Table 1, the values $\Delta H_{f,298}[^{\bullet}CH_2CO_2H] = -59.5 \pm 2.9$ kcal/mol and $D_{298}[HO_2CCH_2{-}H] = 95.3 \pm 2.9$ kcal/mol are derived. Correction for the appropriate differences in 0−298 K integrated heat capacities (obtained from the calculated harmonic vibrational frequencies) gives the corresponding 0 K values: $\Delta H_{f,0}[^{\bullet}CH_2CO_2H] = -58.2 \pm 2.9$ kcal/mol and $D_0[HO_2CCH_2{-}H] = 93.3 \pm 2.9$ kcal/mol (Table 1). The 298 K bond energy found in this work is between two other experimental values that were reported recently. In a photoionization study, Orlov *et al.*[34] obtained $\Delta H_f[^{\bullet}CH_2CO_2H] = -58.1$ kcal/mol on the basis of a measured heat of formation for $^{\bullet}CH_2CO_2Me$ and an estimated methyl substituent effect on the radical stability. This value leads to a (presumably 298 K) bond dissociation energy of 97.3 kcal/mol. Holmes and co-workers report a value of 93.9 ± 3.0 kcal/mol based on electron impact appearance energy measurements.[35] Although some approximations were employed in the photoionization study, the resulting errors are probably not enough to account entirely for the discrepancy between these two values. For example, in the case of methyl acetate, where the heat of formation of the $^{\bullet}CH_2CO_2Me$ radical was measured directly by both groups, the derived C−H bond energies still differ by 4.7 kcal/mol.

Theoretical calculations using small basis sets lead to consistently higher values for the C−H bond energy in acetic acid. Leroy and co-workers[36] carried out MP4 calculations with a 4-31G basis set on a large number of substituted methyl radicals and methanes. They calculated a bond strength of 98.4

(34) Orlov, V. M.; Misharev, A. D.; Takhistov, V. V.; Ryabinkin, I. I. *Iz. Akad. Nauk. SSSR, Ser. Khim.* **1988**, *7*, 1514.
(35) Holmes, J. L.; Lossing, F. P.; Mayer, P. M. *J. Am. Chem. Soc.* **1991**, *113*, 9723.
(36) Leroy, G.; Sana, M.; Wilante, C. *J. Mol. Struct. (THEOCHEM)* **1991**, *228*, 37.

kcal/mol on the basis of an isodesmic reaction that included methyl radical and methane. Pasto and co-workers obtained a value of 99.2 kcal/mol using a similar isodesmic reaction approach with an ROHF/4-31G procedure.[37]

Summary

The acetate radical anion **1** has been generated at room temperature in the gas phase from the reaction of F_2 with the enolate ions of either acetic acid or trimethylsilyl acetate. This cross-conjugated radical anion undergoes characteristic ion/molecule reactions with NO, NO_2, and SO_2 by transfer of a $CH_2^{\bullet-}$ group and with CH_3SSCH_3 by methylthio group abstraction. Although hydrogen atom and halogen atom abstraction reactions by **1** are not observed to occur with hydrocarbons and alkyl halides, hydrogen atom transfer does occur during formation of cluster ions of **1** with carboxylic acids. Collision-induced dissociation of **1** produces $CH_2^{\bullet-} + CO_2$ with a measured threshold energy (D_0) of 2.64 ± 0.12 eV. This is comparable to the known decarboxylation energy of $CH_3CO_2^-$ (2.45 ± 0.13 eV). The (oxygen) proton affinity of **1** ($\Delta H_{acid}(^{\bullet}CH_2CO_2H)$) has been determined to be 347.0 ± 1.1 kcal/mol from the kinetic method. These data have been used in conjunction with thermochemical cycles and additional thermochemical data from the literature to derive absolute heats of formation for **1** and $^{\bullet}CH_2CO_2H$, as well as C−H bond strengths in acetate ion and acetic acid (Table 1). The α-acetic acid radical ($^{\bullet}CH_2CO_2H$) is found to be a stronger acid than acetic acid by 1.6 kcal/mol, while the acetate ion is found to have a slightly weaker C−H bond than that in acetic acid.

Acknowledgment. We are grateful to Professor R. G. Cooks for helpful comments. This work was supported by the National Science Foundation and the Department of Energy, Office of Basic Sciences. P.G.W. is grateful to Lubrizol Corporation for a fellowship.

Appendix: Calculation of Uncertainties in Acid−Base Properties Determined by the Kinetic Method

The uncertainties in acid−base properties determined by the kinetic method are often left unspecified, arbitrarily assigned, or simply taken to be equal to the error in the slope and intercept of the semilog calibration plots. Actually, the absolute uncertainties in the derived acidities or proton affinities arising from nonsystematic effects are determined by both the quality of the linear regression used for the calibration and the uncertainties in the reference data used to construct the calibration plot. In the following, we provide an analysis of these two contributions and recommend a simple procedure for calculating the absolute errors associated with kinetic method measurements. The methods described here, based on the analyses recommended by Bevington,[38] address the question of random errors in kinetic method measurements. Systematic effects on the CID yield ratio measurements and systematic errors in the reference data used for the calibrations will also contribute to the absolute uncertainty.

For a regression equation of the form $Y_i = a + bX_i$, the uncertainties in the regression parameters a and b are given by σ_a and σ_b, respectively. These are calculated from the uncertainties in X_i and Y_i, denoted by σ_{X_i} and σ_{Y_i}, using eqs A.1 and A.2, respectively, where $\Delta = [\sum(1/\sigma_i^2)][\sum(X_i^2/\sigma_i^2)] - [\sum(X_i/\sigma_i^2)]^2$ and $\sigma_i^2 = b^2\sigma_{X_i}^2 + \sigma_{Y_i}^2$. The quality of the fit is indicated by the value of χ^2. This is calculated using eq A.3.

$$\sigma_a^2 = [\sum(X_i^2/\sigma_i^2)]/\Delta \quad (A.1)$$

$$\sigma_b^2 = [\sum(1/\sigma_i^2)]/\Delta \quad (A.2)$$

$$\chi^2 = \sum[(Y_i - a - bX_i)^2/\sigma_i^2] \quad (A.3)$$

For a given χ^2 and number of degrees of freedom, $\nu = N - 2$, where N refers to the number of points used in the regression, the probability that the data, Y_i and X_i, are described by the relation $Y_i = (a \pm \sigma_a) + (b \pm \sigma_b)X_i$ is given by $1 - P(\chi^2,\nu)$, where P is the Γ-distribution function shown in eq A.4. If the

$$P(\chi^2,\nu) = (\chi^2)^{(\nu-2)/2} \exp(-\chi^2/2)/\Gamma(\nu/2) \quad (A.4)$$

χ^2 probability, $1 - P$, is "too low", i.e. near 0, then the uncertainties in X_i and Y_i need to be increased and σ_a and σ_b will increase accordingly. Similarly, if $1 - P$ is "too high", i.e. near 1, then σ_{X_i} and σ_{Y_i} can be decreased, with a corresponding decrease in σ_a and σ_b.

For the kinetic method experiments using the multireference calibration approach described in this paper, Y_i refers to $\Delta G_{acid}(RCO_2H)$, X_i represents ln R, b is the factor $-RT$, and a is $\Delta G_{acid}(^{\bullet}CH_2CO_2H)$. It follows directly that the uncertainty for an acidity determined using the multireference approach, σ_{acid}, is equal to σ_a, calculated according to eq A.1. For the single-reference calibration approach and the "global" calibration approach, the unknown acidity is determined from the full regression equation, so both σ_a and σ_b are involved in the final uncertainty. Also included is the uncertainty in the measured ratio, R, for the compound with the unknown acidity. Statistical combination of these component uncertainties results in eq A.5,

$$\sigma_{acid}^2 = \sigma_a^2 + (b \ln R)^2[\sigma_b^2/b^2 + \sigma_{\ln R}^2/(\ln R)^2] \quad (A.5)$$

where σ_a and σ_b are calculated according to eqs A.1 and A.2, respectively, and $\sigma_{\ln R}$ is given by the fractional uncertainty $\sigma_{\ln R} = \sigma_R/R$. The uncertainties in the gas-phase acidity of $^{\bullet}CH_2CO_2H$ obtained using the kinetic method with both the single-reference and multireference approaches, along with the corresponding χ^2 probabilities, are listed in Table 2.

Table 2. Derived Error Limits and χ^2 Probabilities for Kinetic Method Measurements

single-reference approach		multireference approach	
$\Delta G_{acid}(^{\bullet}CH_2CO_2H)^{a,b}$	$1 - P(\chi^2,\nu)^d$	$\Delta G_{acid}(^{\bullet}CH_2CO_2H)^{a,c}$	$1 - P(\chi^2,\nu)^d$
339.9 ± 1.0	1.000	340.1 ± 1.0	0.994
339.9 ± 0.3	0.994	340.1 ± 0.7	0.981
339.9 ± 0.2	0.957	340.1 ± 0.6	0.957

[a] Values in kcal/mol. [b] Uncertainty calculated according to eq A.5. [c] Uncertainty calculated according to eq A.1. [d] Calculated from the experimental data using eq A.4.

The decision as to what constitutes "too high" or "too low" a probability is left to the discretion of the investigator and, therefore, is fairly arbitrary. While some may insist that the probabilities should be greater than 0.99, others may be satisfied with probabilites as low as 0.10. Accordingly, we have developed a means to calculate the uncertainties for the kinetic method that do not require any arbitrary decisions regarding the acceptable limits.

The uncertainties for the acidities reported in this work due to nonsystematic effects include the errors due to the uncertainty in the data points, calculated using eqs A.1 and A.2, respectively, as well as the the statistical uncertainties due to variance in the

(37) Pasto, D. J.; Krasnansky, R.; Zercher, C. *J. Org. Chem.* **1987**, *52*, 3062.

(38) Bevington, P. R. *Data Reduction and Error Analysis for the Physical Sciences*; McGraw-Hill: New York, 1969.

data. The variance in the data, s^2, can be calculated from χ^2 according to eq A.6. The uncertainties in a and b due to the

$$s^2 = (N/(N-2))\chi^2/\sum(1/\sigma_i^2) \quad \text{(A.6)}$$

variance of the data, σ_{av} and σ_{bv}, are estimated using eqs A.7 and A.8, respectively, where $\Delta' = N\sum X_i^2 - (\sum X_i)^2$. The overall uncertainties in a and b, denoted by σ'_a and σ'_b, can now be

$$\sigma_{av}{}^2 = s^2\sum X_i^2/\Delta' \quad \text{(A.7)}$$

$$\sigma_{bv}{}^2 = Ns^2/\Delta' \quad \text{(A.8)}$$

calculated from the two component uncertainties using eqs A.9 and A.10, respectively. The uncertainties assigned to the acid-

$$\sigma'_a{}^2 = \sigma_a{}^2 + \sigma_{av}{}^2 \quad \text{(A.9)}$$

$$\sigma'_b{}^2 = \sigma_b{}^2 + \sigma_{bv}{}^2 \quad \text{(A.10)}$$

ities determined in this work are calculated using this method and are comparable to those with the highest probabilities in Table A.1.